

# A Dual-Band Rectenna Using Broadband Yagi Antenna Array for Ambient RF Power Harvesting

Hucheng Sun, Yong-xin Guo, *Senior Member, IEEE*, Miao He, and Zheng Zhong

**Abstract**—This letter presents a dual-band rectenna that can harvest ambient RF power of GSM-1800 and UMTS-2100 bands efficiently. The novel rectenna is based on a broadband  $1 \times 4$  quasi-Yagi antenna array with bandwidth from 1.8 to 2.2 GHz and high gains of 10.9 and 13.3 dBi at 1.85 and 2.15 GHz, respectively. Also, a dual-band rectifier that can sufficiently enhance the RF-to-dc power conversion efficiency (PCE) at ambient RF power level is designed for the rectenna. Measurement results show that a PCE of 40% and an output dc voltage of 224 mV have been achieved over a 5-k $\Omega$  resistor when the dual-tone input power density is 455  $\mu\text{W}/\text{m}^2$ . Additionally, output dc voltage varying between 300–400 mV can be obtained by collecting the relatively low ambient RF power.

**Index Terms**—Antenna array, energy harvesting, rectenna, rectifier, Yagi–Uda antenna.

## I. INTRODUCTION

RECENT advances in RF energy-harvesting technology have made self-sustainable devices feasible. The major concern for these devices is typically the battery life and replacement. Applying RF energy-harvesting technique to them can significantly extend the battery life and sometimes even avoid the need for a battery. The ambient RF power is a good potential candidate for the energy supply as it is widely broadcast from numerous reliable electromagnetic resources. However, since the power density of the ambient RF power is extremely small, it is very challenging to design RF energy-harvesting systems with satisfying RF-to-dc power conversion efficiencies (PCEs).

The key element of an RF energy-harvesting system is the rectenna [1], which is a combination of an antenna and a rectifier. The antenna receives the RF power, and the rectifier converts it into dc power. A few rectennas in the prior literature have been designed for harvesting the ambient RF energy. A 550-MHz rectenna [2] for Digital TV (DTV) energy harvesting exhibited efficiency of 18.2% with input power of  $-20$  dBm. Another rectenna [3] with a boost converter showed a voltage of 2.78 V with input power of 5 dBm at a distance of 10 m from the cell tower. However, in the above referenced articles,

TABLE I  
MEASURED AMBIENT POWER DENSITIES OF DIFFERENT PUBLIC TELECOMMUNICATION BANDS

Band	Downlink Frequency (MHz)	Antenna Gain (dBi)	Received Power* (dBm)	Power Density ( $\mu\text{W}/\text{m}^2$ )
GSM-900	925-960	2	-35 - -25	23.8 - 256.7
GSM-1800	1805-1880	10	-25 - -15	143.9 - 1560.6
UMTS-2100	2110-2170	10	-25 - -15	196.6 - 2079.2

\*The distance and height from the nearest cell tower to the receiving horn antenna are 150 m and 11.8 m respectively. The receiving horn antenna is directly pointed to the cell tower.

rectennas can only perform for narrow band, so they cannot fully utilize the RF power in the ambience. In [4], rectifiers were connected to broadband antennas to collect RF energy over a broad frequency band. However, the maximum efficiency can only reach 20% at 3 GHz with relatively high input power density of 62  $\mu\text{W}/\text{cm}^2$ . Hence, this rectenna is actually incapable of harvesting the ambient RF energy.

In this letter, a dual-band rectenna with high RF-to-dc PCE for ambient RF energy harvesting is proposed. In order to make the best use of the ambient RF energy in each frequency band, the power densities of ambient RF energy available from public telecommunication services have been first investigated using a wideband standard horn antenna (0.8–18 GHz) and a spectrum analyzer on the campus of the National University of Singapore, Singapore. From the measured results, it can be found that only the power of the downlink channels in three bands, GSM-900, GSM-1800, and UMTS-2100, is dominant among the ambient RF energy; their details are shown in Table I. The related power densities are calculated as the received power divided by the antenna's effective aperture size. Additionally, the total RF power of all ambient communication bands is measured by the wideband horn antenna and a power meter. The value varies from  $-15$  to  $-10$  dBm, which is much larger than the summation of the received power in the three bands listed in the Table I, revealing the possibility and potential of ambient RF power harvesting. It can also be found from Table I that the power densities of GSM-1800 and UMTS-2100 bands are apparently much larger than that of the GSM-900 band. Therefore, considering the tradeoff between the rectenna size and its received power, the proposed rectenna in this letter primarily focuses on GSM-1800 and UMTS-2100 bands.

## II. QUASI-YAGI ANTENNA ARRAY

Due to the size limitation of the fabrication, the design starts from a  $1 \times 2$  subarray. Fig. 1(a) and (b) gives the top and side views of the proposed quasi-Yagi subarray, which is fabricated

Manuscript received January 30, 2013; revised April 11, 2013; accepted June 20, 2013. Date of publication July 11, 2013; date of current version August 05, 2013. This work was supported by the Singapore Ministry of Education Academic Research Fund Tier 1 under Project R-263-000-667-112.

The authors are with the Department of Electrical and Computer Engineering, National University of Singapore, Singapore 117576, Singapore (e-mail: eleguoyx@nus.edu.sg).

Color versions of one or more of the figures in this letter are available online at <http://ieeexplore.ieee.org>.

Digital Object Identifier 10.1109/LAWP.2013.2272873

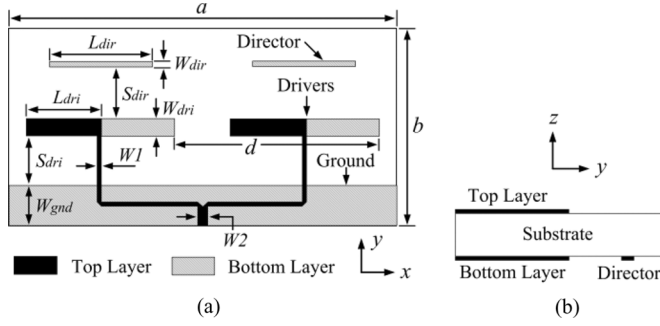
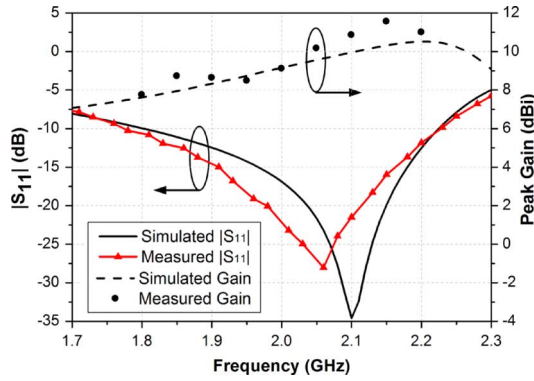


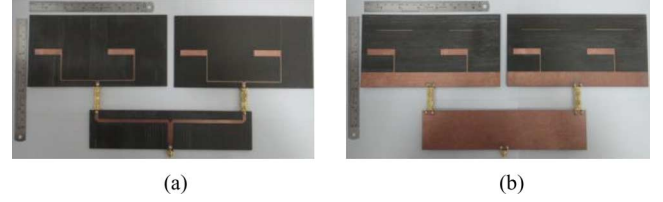
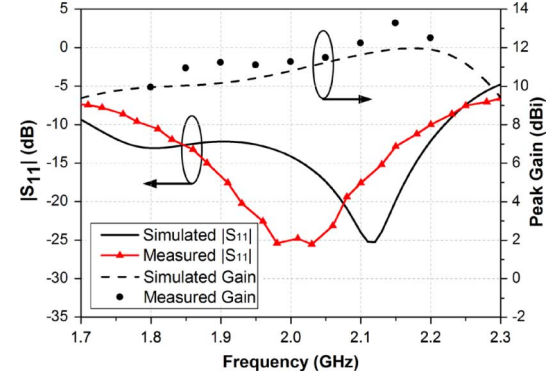
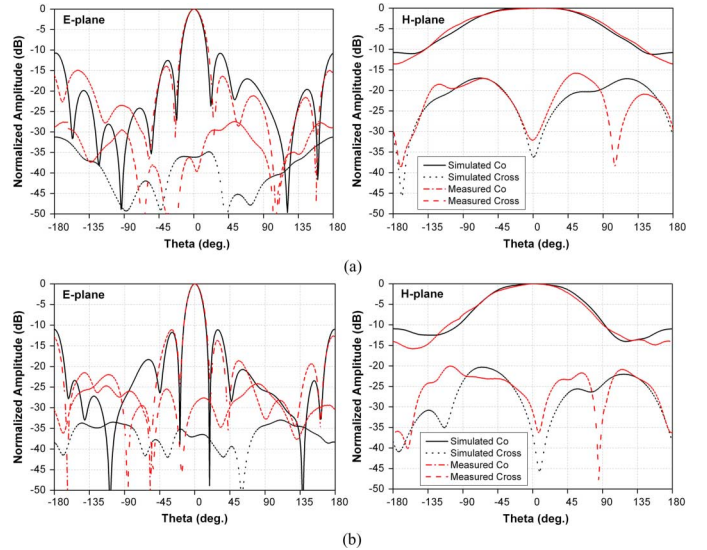
Fig. 1. Layout of the quasi-Yagi subarray. (a) Top view. (b) Side view.

Fig. 2. Simulated and measured  $|S_{11}|$  and gain of the  $1 \times 2$  subarray.

on a 62-mil-thick RT/Duroid 5870 substrate with a dielectric constant of 2.33. The top and bottom metallization comprises a microstrip feedline, two double-sided parallel-strip feedlines, two dipole elements (drivers), two directors, and a conductor plane. The conductor plane can be treated as a virtual ground plane and acts as the reflector element for the two antenna elements, which makes the subarray radiate forward and obtain a good front-to-back ratio [5]. Using the microstrip feedline, the extra balun as a part of the feed network, required in the conventional microstrip quasi-Yagi antenna [5], can be avoided.

In the design, the High Frequency Structure Simulator (HFSS) was used to optimize the subarray. As with the classic Yagi-Uda antenna, proper design requires careful optimization of the driver, director, and reflector parameters, which include element spacing, length, and width. The initial lengths of the directors and drivers are chosen to be approximately a half-wavelength at the center frequency. After optimization, the subarray's parameters are (unit: millimeter):  $a = 190$ ,  $b = 100$ ,  $W_1 = 1.2$ ,  $W_2 = 4.4$ ,  $W_{\text{gnd}} = 20$ ,  $L_{\text{dri}} = 37$ ,  $W_{\text{dri}} = 8$ ,  $L_{\text{dir}} = 50$ ,  $W_{\text{dri}} = 0.5$ ,  $S_{\text{dir}} = 26$ ,  $S_{\text{dri}} = 24$ ,  $d = 100$ . Fig. 2 plots the simulated and measured  $|S_{11}|$  and gain of this subarray. The measured  $-10$ -dB bandwidth is from 1.78 to 2.22 GHz, while the measured gain is 7.8–11.5 dBi over this frequency range.

A  $1 \times 4$  quasi-Yagi array can be formed by simply connecting two  $1 \times 2$  subarrays together with a T-junction power divider. The photographs of the  $1 \times 4$  array are shown in Fig. 3. The distance between each element is equal to that of the previous subarray. In this way, the array has more flexibility to switch between the  $1 \times 4$  and  $2 \times 2$  topologies. The simulated and measured  $|S_{11}|$  and gain of the  $1 \times 4$  array are illustrated in Fig. 4.

Fig. 3. Photographs of the  $1 \times 4$  quasi-Yagi array. (a) Top side. (b) Back side.Fig. 4. Simulated and measured  $|S_{11}|$  and gain of the  $1 \times 4$  quasi-Yagi array.Fig. 5. Simulated and measured E-plane and H-plane patterns at (a) 1.85 and (b) 2.15 GHz for the  $1 \times 4$  quasi-Yagi array.

It can be seen that the measured  $-10$ -dB bandwidth is from 1.8 to 2.2 GHz (20%), which can still cover the GSM-1800 and UMTS-2100 bands. High gain of 9.9–13.3 dBi has been achieved over the entire band, with 10.9 and 13.3 dBi at 1.85 and 2.15 GHz, respectively. Since the effective aperture area of an antenna is proportional to its gain, the use of a high-gain antenna is able to receive more power for rectification to a large extent. Fig. 5 gives the simulated and measured E- and H-plane patterns at 1.85 and 2.15 GHz for the  $1 \times 4$  array. Good agreement can be seen from the comparison between the measured and simulated values. Also, the cross-polarization level in each plane is low. In addition, broad beamwidths have been observed in H-planes. The half-power beamwidths (HPBW) are about  $170^\circ$  and  $110^\circ$  at 1.85 and 2.15 GHz, respectively, which are

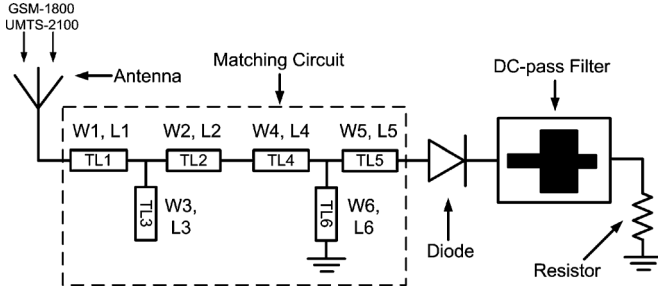


Fig. 6. Topology of the proposed rectifier.

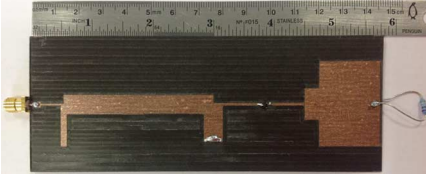


Fig. 7. Photograph of the fabricated rectifier.

benefits as the alignment of the rectenna does not need to be very precise to keep the PCE constant.

### III. RECTIFIER DESIG AND MEASUREMENT

The entire topology of the proposed rectifier is illustrated in Fig. 6. The substrate used is 31-mil-thick RT/Duroid 5880 with dielectric constant of 2.2. In this design, the series-mounted diode topology is adopted since it tends to have a higher efficiency under low-input RF power conditions [6]. As shown in Fig. 6 from TL1 to TL6, a two-section T-shape microstrip transformer [7] is used to achieve the dual-band characteristic so that the two bandwidths can be enhanced, and the optimized widths of the microstrip lines are not too wide or too narrow. To provide a dc-patch in the circuit, the microstrip line TL6 is grounded by via-holes. A Schottky diode Avago HSMS-2852 ( $V_{th} = 150$  mV,  $C_j = 0.18$  pF,  $R_s = 25$   $\Omega$ ) is inserted between the matching circuit and the dc-pass filter to convert the microwave power into dc power. The dc-pass filter is realized by a simple stepped-impedance microstrip line low-pass filter, followed by a resistive load to extract the dc power.

The parameters of the matching circuit, dc-pass filter, and the resistive load can be initially calculated and then optimized in the software Advanced Design System (ADS) by setting appropriate goals. At the first stage, a preliminary rectifier containing only a diode, a dc-pass filter, and a resistor was optimized under low input power with the goal of high efficiency at both 1.84 and 2.14 GHz. In this way, the optimal dc-pass filter and the load resistance was obtained. After that, the matching circuit was optimized separately to match the input impedance of the rectifier to 50  $\Omega$  at both 1.84 and 2.14 GHz. The optimized parameters are (unit: millimeter):  $W1 = 0.6$ ,  $L1 = 8.3$ ,  $W2 = 7.8$ ,  $L2 = 23.5$ ,  $W3 = 2.5$ ,  $L3 = 13.3$ ,  $W4 = 7.5$ ,  $L4 = 25.3$ ,  $W5 = 0.9$ ,  $L5 = 16.7$ ,  $W6 = 7.7$ ,  $L6 = 10.8$ . The load resistance is 5 k $\Omega$ . Fig. 7 shows the photograph of the fabricated rectifier.

Fig. 8 plots the measured return losses of the rectifier at different input power levels. It can be found that good impedance matching is achieved at 1.84 and 2.14 GHz, proving the capability of the dual-frequency matching circuit. The

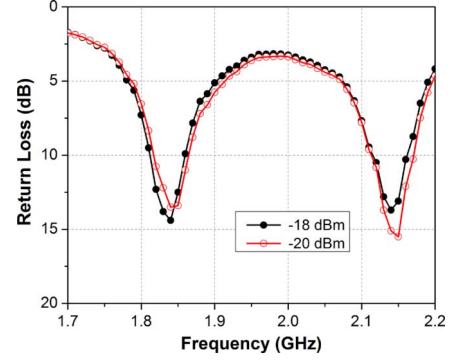


Fig. 8. Measured return losses of the rectifier at different input power levels.

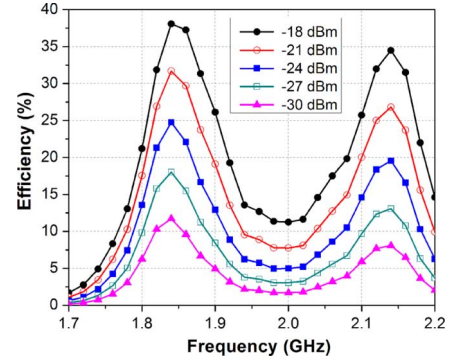


Fig. 9. Measured efficiencies of the rectifier against frequency at different input power levels.

frequency-dependent characteristic of the rectifier's conversion efficiency is investigated at different power levels ( $-30$  to  $-18$  dBm), illustrated in Fig. 9. The measured conversion efficiency can be obtained by

$$\eta(\%) = \frac{V_L^2}{R_L} \times \frac{1}{P_{in}} \times 100 \quad (1)$$

where  $V_L$  is the output dc voltage on the resistor,  $R_L$  is the resistance value, and  $P_{in}$  is the power level of the single-tone input signal generated by a signal generator. It can be seen from Fig. 9 that higher efficiencies can be achieved in the frequency ranges of 1.81–1.87 and 2.11–2.17 GHz, revealing the rectifier's capability to harvest the RF power in the GSM-1900 and UMTS-2100 bands.

In fact, the input power to the rectenna can be regarded as multitone when measuring in the ambience since the ambient RF power is distributed over the two bands. To demonstrate that the multitone input of the same power level can enhance the efficiency of the rectifier, measured efficiencies of the rectifier with single- and dual-tone input are plotted in Fig. 10. For single-tone input, the efficiency at 1.84 GHz can reach 34% at input power of  $-20$  dBm and can still remain 22.3% when the input power decreases to  $-25$  dBm. For the dual-tone measurement, the two equal-power tones at 1.84 and 2.14 GHz are generated from two signal generators and summed up by a power combiner (ZFRSC-42), then input to the rectifier. The total power of the two tones is counted as the input power. It can be seen from Fig. 10 that the efficiency can be improved in this way. Hence, this fact implies that this dual-band rectifier can harvest the dispersed RF power separated in different channels of the

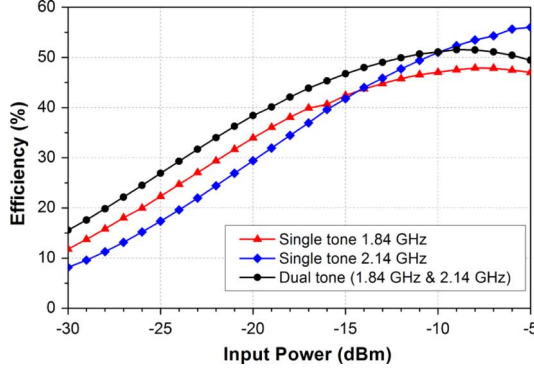


Fig. 10. Measured efficiencies of the rectifier by using single and dual tones.

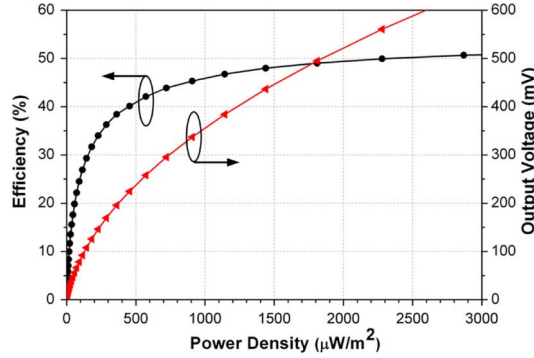


Fig. 11. Measured efficiency and output voltage of the rectifier against power density with dual-tone (1.84 and 2.14 GHz) input.

GSM-1800 and UMTS-2100 bands at the same time with considerably higher conversion efficiency.

To gain a better understanding of the rectenna's (antenna plus rectifier) efficiency performance and pave the way for the following measurement in the ambience, the dual-tone curve of Fig. 10 is redrawn in Fig. 11. The power density is calculated as

$$\begin{aligned} \text{P.D.} &= \frac{P(f_1) + P(f_2)}{A_{\text{eff}}(f_1) + A_{\text{eff}}(f_2)} \\ &= \frac{4\pi}{c^2} \frac{P(f_1) + P(f_2)}{G(f_1)/f_1^2 + G(f_2)/f_2^2} \end{aligned} \quad (2)$$

where  $P$  is input power level,  $A_{\text{eff}}$  is antenna's equivalent aperture area,  $G$  is measured gain of the antenna,  $c$  is speed of light,  $f_1$  equals 1.84 GHz, and  $f_2$  equals 2.14 GHz. From calculation, the overall efficiency keeps higher than 40% when the power density is more than  $455 \mu\text{W}/\text{m}^2$ . Additionally, for power density of  $181 \mu\text{W}/\text{m}^2$ , the overall conversion efficiency has still remained 29.3%. The output dc voltage of the rectenna always goes up with increasing input power density.

#### IV. RECTENNA MEASUREMENT IN THE AMBIENCE

As shown in Fig. 12, the rectenna's capability of recycling ambient RF power has been tested on the rooftop (the same place as measuring the receiving power by a horn in Table I), which is so high that no buildings around shield the visual field, and so empty that no irrelevant radiating sources nearby affect the measurement. The output dc voltage was measured to vary between 300 to 400 mV most of the time, and it could also reach more than 400 mV sometimes due to the variation of ambient

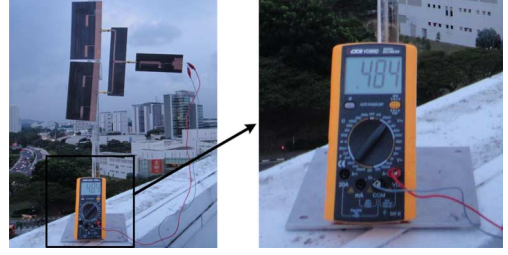


Fig. 12. Photographs of (left) the experimental setup for the rectenna measurement in the ambience and (right) the indication of the voltmeter.

RF energy, e.g., 484 mV as shown in Fig. 12. Based on the measured ambient RF power densities of GSM-1800 and UMTS-2100 bands listed in Table I, the corresponding efficiency of this dual-band rectenna is estimated to be above 16.6%–43%, demonstrating that the proposed rectenna would be profitably applied to harvesting ambient RF energy of GSM-1800 and UMTS-2100 bands. It is worth noting that the efficiency can reach ~50% if a power level of  $\sim -10$  dBm is received from a dedicated power source.

#### V. CONCLUSION

A new rectenna with broadband  $1 \times 4$  quasi-Yagi antenna array and a dual-band rectifier has been designed to harvest the ambient RF power of GSM-1800 and UMTS-2100 bands. It has exhibited an output dc voltage varies between 300 to 400 mV when measured in the ambience. As many sensors monitor physical quantities not frequently, their duty cycle of operation and average power requirement are low [8]. Hence, with a suitable energy management circuit, many sensor systems can be operational by harvesting ambient RF power using this proposed rectenna. Since the ambient RF energy harvesting is emerged as an urgent and challengeable issue in the creation of wireless sensor networks that depend on truly autonomous devices, this study can be treated as a very pointed attempt in this respect.

#### REFERENCES

- [1] J. A. G. Akkermans, M. C. van Beurden, G. J. N. Doodeman, and H. J. Visser, "Analytical models for low-power rectenna design," *IEEE Antennas Wireless Propag. Lett.*, vol. 4, pp. 187–190, 2005.
- [2] C. Mikeka, H. Arai, A. Georgiadis, and A. Collado, "DTV band micropower RF energy-harvesting circuit architecture and performance analysis," in *IEEE Int. Conf. RFID-TA. Dig.*, 2011, pp. 561–567.
- [3] M. Arrawatia, M. S. Baghini, and G. Kumar, "RF energy harvesting system from cell towers in 900 MHz band," in *Proc. Nat. Conf. Commun.*, Bangalore, India, 2011, pp. 1–5.
- [4] J. A. Hagerty, F. B. Helmbrecht, W. H. McCalpin, R. Zane, and Z. B. Popovic, "Recycling ambient microwave energy with broad-band rectenna arrays," *IEEE Trans. Microw. Theory Tech.*, vol. 52, no. 3, pp. 1014–1024, Mar. 2004.
- [5] N. Kaneda, W. R. Deal, Y. Qian, R. Waterhouse, and T. Itoh, "A broad-band planar quasi-Yagi antenna," *IEEE Trans. Antennas Propag.*, vol. 50, no. 8, pp. 1158–1160, Aug. 2002.
- [6] V. Marian, C. Vollaie, J. Verdier, and B. Allard, "Potentials of an adaptive rectenna circuit," *IEEE Antennas Wireless Propag. Lett.*, vol. 10, pp. 1393–1396, 2011.
- [7] M. A. Nikravan and Z. Atlasbaf, "T-section dual-band impedance transformer for frequency-dependent complex impedance loads," *Electron. Lett.*, vol. 47, pp. 551–553, May 2011.
- [8] U. Olgun, C.-C. Chen, and J. L. Volakis, "Design of an efficient ambient WiFi energy harvesting system," *Microw. Antennas Propag.*, vol. 6, no. 11, pp. 1200–1206, Nov. 2012.